

Nanostructured Microcantilevers with Functionalized Cyclodextrin Receptor Phases: Self-Assembled Monolayers and Vapor-Deposited Films

Christopher A. Tipple,[†] Nickolay V. Lavrik,[†] Mustafa Culha,[†] Jeremy Headrick,[†] Panos Datskos,^{†,‡} and Michael J. Sepaniak^{*,†}

The University of Tennessee, Knoxville, and Oak Ridge National Laboratory

It is shown that the performance of microcantilever-based chemical sensors in a liquid environment is affected by altering cantilever surface morphology and receptor phase type and thickness. Self-assembled monolayers of thiolated β -cyclodextrin (HM- β -CD) and thin films of vapor-deposited heptakis (2,3-*O*-diacetyl-6-*O*-tertbutyl-dimethylsilyl)- β -cyclodextrin (HDATB- β -CD) were studied on smooth and nanostructured (dealloyed) gold-coated microcantilever surfaces. The dealloyed surface contains nanometer-sized features that enhance the transduction of molecular recognition events into cantilever response, as well as increase film stability for thicker films. Improvements in the limits of detection of the compound 2,3-dihydroxynaphthalene as great as 2 orders of magnitude have been achieved by manipulating surface morphology and film thickness. The observed response factors for the analytes studied varied from 0.02–604 nm/ppm, as determined by cantilever deflection. In general, calibration plots for the analytes were linear up to several hundred nanometers in cantilever deflections.

Microfabricated cantilevers have traditionally found utility in atomic force microscopy (AFM) imaging. During the past decade, however, microcantilevers (MCs) have been increasingly used as transducers in chemical sensing systems.^{1–10} Their increased use

has been due to a few key advantages that MCs have over more traditional transducers, such as surface acoustic wave (SAW) or quartz crystal microbalance (QCM) devices. For example, MCs are well-suited for miniaturization and can be used as elements in sensor arrays.^{11–13} These arrays lead to a higher degree of selectivity than can be achieved using a single cantilever because of the use of multiple chemically selective coatings. Another unique feature of these ultrathin MCs is that they possess an extremely high surface-to-volume ratio. Thus, changes in the conditions on or near the surface resulting from chemical species present in the environment of the MC can significantly modulate surface stress. This can result in bending (the most commonly measured response of MCs) if opposite sides of the cantilever are modulated by different degrees. When using MCs as chemical sensors, this differential modulation is generally assured by using asymmetric MCs wherein one side of the cantilever preferentially interacts with the target analyte(s) via surface adsorption or absorption into a thin chemical film on the surface. The surface of the opposite side is largely passive relative to the chemically treated side for these asymmetric MCs. According to Stoney,¹⁴ the tip deflection, z_{\max} , of a smooth-surface cantilever resulting from differential stress at its opposing sides, $\Delta\sigma$, is given by eq 1,

$$z_{\max} = \frac{3l^2(1-\nu)}{Et^2}\Delta\sigma \quad (1)$$

where ν and E are, respectively, the Poisson's ratio and Young's modulus for the cantilever, and l and t are its length and thickness, respectively.

Recent reports from several research groups^{1–13} confirm that sensors based on MCs have a substantial potential for various

[†] The University of Tennessee.

[‡] Oak Ridge National Laboratory.

- (1) Raiteri, R.; Nelles, G.; Butt, H.-J.; Knoll, W.; Skladal, P. *Sens. Actuators B* **1999**, *61*, 213–217.
- (2) Boisen, A.; Thaysen, J.; Jensenius, H.; Hansen, O. *Ultramicroscopy* **2000**, *82*, 11–16.
- (3) Ji, H.-F.; Hansen, K. M.; Hu, Z.; Thundat, T. *Sens. Actuators B* **2001**, *72*, 233–238.
- (4) Luginbuhl, P.; Racine, G.-A.; Lerch, P.; Romanowicz, B.; Brooks, K. G.; Rooij, N. F. d.; Renaud, P.; Setter, N. *Sens. Actuators A* **1996**, *54*, 530–535.
- (5) Jensenius, H.; Thaysen, J.; Rasmussen, A. A.; Veje, L. H.; Hansen, O.; Boisen, A. *Appl. Phys. Lett.* **2000**, *76*, 2615–2617.
- (6) Lavrik, N. V.; Tipple, C. A.; Datskos, P. G.; Sepaniak, M. J. *Biomed. Microdevices* **2001**, *3*, 35–44.
- (7) Fritz, J.; Baller, M. K.; Lang, H. P.; Rothuizen, H.; Vettiger, P.; Meyer, E.; Guntherodt, H.-J.; Gerber, C.; Gimzewski, J. K. *Science* **2000**, *288*, 316–318.
- (8) Fagan, B.; Tipple, C. A.; Xue, B.; Datskos, P.; Sepaniak, M. *Talanta* **2000**, *53*, 599.
- (9) Datskos, P. G.; Sepaniak, M. J.; Tipple, C. A.; Lavrik, N. *Sens. Actuators B* **2001**, *76*, 393–402.

- (10) Betts, T. A.; Tipple, C. A.; Sepaniak, M. J.; Datskos, P. G. *Anal. Chim. Acta* **2000**, *422*, 89.
- (11) Baller, M. K.; Lang, H. P.; Fritz, J.; Gerber, C.; Gimzewski, J. K.; Drechsler, U.; Rothuizen, H.; Despont, M.; Vettiger, P.; Battiston, F. M.; Ramseyer, J.-P.; Fornaro, P.; Meyer, E.; Guntherodt, H.-J. *Ultramicroscopy* **2000**, *82*, 1–9.
- (12) Maute, M.; Raible, S.; Prins, F. E.; Kern, D. P.; Weimar, U.; Gopel, W. *Microelectron. Eng.* **1999**, *46*, 439–442.
- (13) Britton, C. L.; Jones, R. L.; Oden, P. I.; Hu, Z.; Warmack, R. J.; Smith, S. F.; Bryan, W. L.; Rochelle, J. M. *Ultramicroscopy* **2000**, *82*, 17–21.
- (14) Stoney, G. G. *Proc. R. Soc. London* **1909**, *A82*, 172–177.

analytical applications. To fully realize this potential, however, further optimization of MCs designs may be required. A clean, smooth, solid surface generally exhibits a tensile (positive) surface stress due to the electronic arrangement of the atoms composing the surface and, significantly, changes in stress on that surface can occur when the surface atoms are caused to rearrange as a result of adsorption by a chemical species.¹⁵ The change in stress can be either compressive (negative) or tensile, depending upon the nature of the adsorbed species. The surface stress and surface free energy are related by the Shuttleworth equation (eq 2),

$$\sigma = \gamma + \frac{d\gamma}{d\epsilon_e} \quad (2)$$

where σ is the surface stress, γ is the surface free energy, and ϵ_e is the elastic surface strain that is defined as dA/A where A is the surface area and dA is the elastic increase in surface area.^{15–17} In principle, the second term can be comparable to the surface free energy and assume a positive or negative value.¹⁷ However, a general trend is that if the initial surface free energy is large, then modulation in surface stress and, hence, MC response can be large. For example, pure gold surfaces in contact with air have large surface free energies, typically exceeding 1 N m^{-1} . Not surprisingly, when MCs coated on one side with gold are exposed to alkylthiols in the gas phase, very large total responses are observed as the thiol compounds covalently bond to the gold.^{18,19}

To impart selectivity when MCs are used in analytical sensing, chemically selective receptor phases (e.g., self-assembled monolayers, SAM) are immobilized on one of the sides of the cantilever. Ideally, the interaction of the analyte with the receptor phase, while being selective, is reversible and exhibits reasonable kinetics for sensing applications. The use of MCs with reversible receptor phases for measurements in liquids (e.g., aqueous solutions) has not received a great deal of attention. In part, this is because organic receptor phases in water possess surface free energies that are more than an order of magnitude smaller than the gold–gas-phase case mentioned above. Therefore, modulation of surface stress is small and often within an order of magnitude of the inherent noise of MCs mounted in aqueous environments.⁶ This gives rise to low signal-to-noise levels and somewhat limited dynamic range.

We report herein two approaches to improved performance for liquid-phase measurements using receptor-modified MCs. In both cases, we use cantilevers with nanostructured surfaces to overcome limitations of smooth surfaces. Our idea of MCs with nanostructured surfaces is derived from the models that have been a focus in colloidal science.²⁰ Although our experimental findings indicate that the smooth surface models mentioned above do not strictly apply to the structured MC surfaces, it is also true that classical colloidal models may not fit all the details of these systems.

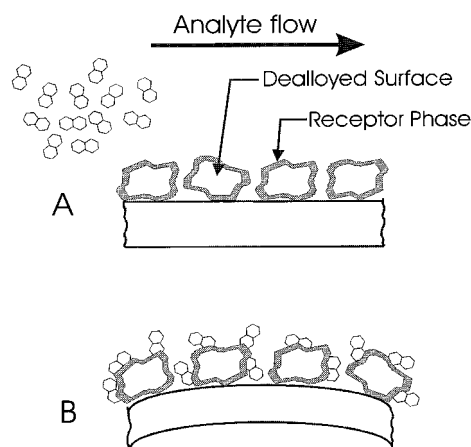


Figure 1. Illustrated depiction of the nanostructured cantilever surface before and after analyte binding.

In the first approach, the limitations of smooth-surface MCs are circumvented via nanostructuring of one side of the cantilever and modifying it with a SAM phase. The nanostructuring increases the available surface for SAM phases and analyte binding and creates a quasi-3-D structure that is colloidal in nature. Importantly, the short-range forces associated with intermolecular interactions in the tight interstitial spaces of colloidal systems can be very large.²⁰ It has also been shown that stresses induced by solvation forces in sol–gels are most pronounced when the interstitial spaces are on the order of several nanometers or smaller.^{21,22} Figure 1 illustrates how analytes binding within sterically confined interstitial spaces may give rise to an enhancement in cantilever bending. The in-plane component of these forces can serve to efficiently convert the chemical energy associated with analyte–receptor binding into MC static bending. In our previous work, gas-phase measurements with nanostructured, cyclodextrin (CD)-modified MCs provided 2 orders of magnitude improvement in chemi-mechanical response (bending) relative to similarly modified smooth MCs.²³

A second method to circumvent the limitations of smooth surfaces is to employ films thicker than SAMs as receptor phases¹⁰ anchored by nanoscale features to a MC surface. Here, in analogy to polymeric phases used previously,^{8,10} the stress that gives rise to bending of the MC results from bulk phase swelling or contractions of the film upon absorption of analyte.^{18,24} There are several forces involved in film swelling, including steric, electrostatic, and hydration forces. The integral force that causes swelling-induced MC bending upon analyte absorption scales with film thickness. In the case of smooth surfaces and weakly adhering receptor phases, however, a large stress gradient generated at the cantilever–coating interface would ultimately result in a stress–slip condition. We demonstrate in this work the advantages of using nanostructured surfaces with nonmonolayer receptor films to reduce stress-related slippage. Films of synthetically modified cyclodextrins (CDs) that are both thinner and thicker than the root-mean-square (RMS) roughness of the supporting

(15) Ibach, H. *Surface Sci. Rep.* **1997**, *29*, 193–263.

(16) Shuttleworth, R. *Proc. Phys. Soc. (London)* **1950**, *63A*, 444–457.

(17) Raiteri, R.; Butt, H.-J.; Grattarola, M. *Electrochim. Acta* **2000**, *46*, 157–163.

(18) Berger, R.; Delamarche, E.; Lang, H. P.; Gerber, C.; Gimzewski, J. K.; Meyer, E.; Güntherodt, H.-J. *Science* **1997**, *276*, 2021–2024.

(19) Datskos, P. G.; Sauers, I. *Sens. Actuators B* **1999**, *61*, 75–82.

(20) Israelachvili, J. *Intermolecular and Surface Forces*, 2nd ed.; Academic Press: San Diego, 1991.

(21) Samuel, J.; Brinker, C. J.; Frink, L. J. D.; Swol, F. v. *Langmuir* **1998**, *14*, 2602–2605.

(22) Frink, L. J. D.; Swol, F. v. *Langmuir* **1999**, *15*, 3296–3301.

(23) Lavrik, N. V.; Tipple, C. A.; Sepaniak, M. J.; Datskos, P. G. *Chem. Phys. Lett.* **2001**, *336*, 371–376.

(24) Hu, Z.; Thundat, T.; Warmack, R. J. *J. Appl. Phys.* **2001**, *90*, 427–431.

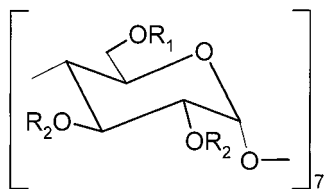


Figure 2. Monomeric units of the functionalized cyclodextrins used as MC receptor phases. R_1 and R_2 for the self-assembled monolayer of HM- β -CD are SH and H, respectively. R_1 and R_2 for the vapor-deposited film of HDATB- β -CD are $(\text{CH}_3)_3\text{CSi}(\text{CH}_3)_3$ and COOCH_3 , respectively.

surface are investigated. To our knowledge, this is the first report of a CD receptor phase that can be vapor-deposited intact on sensor surfaces.

EXPERIMENTAL SECTION

The MCs used in this work were commercially available, V-shaped, $0.55\text{-}\mu\text{m}$ thick, and composed of silicon nitride coated with a $0.05\text{-}\mu\text{m}$ layer of gold (Park Scientific Instruments, Sunnyvale, CA). The length and leg width of the microcantilevers were 350 and 20 μm , respectively. For measurements made using cantilevers coated with smooth gold, the cantilever was cleaned in piranha solution (75% H_2SO_4 , 25% H_2O_2) for 45 s before chemical treatment [Caution: piranha solution reacts violently with organics]. The process of creating the nanostructured MCs having a dealloyed surface is described in greater detail elsewhere.²³ Briefly, the thin gold layer was removed from the commercially obtained cantilevers by immersing them in aqua regia (75% HCl, 25% HNO_3) for 3 min [Caution: aqua regia is very corrosive]. The MCs were then placed into a physical vapor deposition (PVD) chamber (Cooke Vacuum Products, model CVE 301, South Norwalk, CT) to be coated on one side with the appropriate metallic films using thermal deposition. To create a nanostructured MC, a thin film ($\sim 3.5\text{ nm}$) of chromium was applied to the surface to act as an adhesion layer. A thin film of gold ($\sim 15\text{ nm}$) was then applied to the cantilever surface, followed by a film consisting of co-deposited gold and silver. The silver was subsequently chemically removed via oxidation from the film, leaving a gold surface with nanosized, colloid-like features. The thickness of the dealloyed gold layer was $\sim 50\text{ nm}$ in these studies. The smooth MCs were prepared by depositing gold onto the chromium layer until a total thickness of $\sim 50\text{ nm}$ was achieved. These two types of MCs (smooth and nanostructured) were then chemically modified with receptor phases as described below.

The cantilevers used in our studies were chemically modified using two distinct methods. In the first method, a SAM of heptakis-6-mercapto- β -cyclodextrin (HM- β -CD) (see Figure 2) was formed on the cantilever surface. A 1.50 mM solution of HM- β -CD was prepared in 60/40 deaerated DMSO/ H_2O . The MC was then immersed in the HM- β -CD solution for 18–20 h, after which it was rinsed with copious amounts of the DMSO/ H_2O solvent. The chemically treated cantilever was then allowed to soak in the DMSO/ H_2O solution for at least an hour to remove any nonspecifically bound cyclodextrin. The second method involved the physical vapor deposition of the compound heptakis (2,3-*O*-diacetyl-6-*O*-tertbutyl-dimethylsilyl)- β -cyclodextrin (HDATB- β -CD) (see Figure 2) onto the cantilever surface. The HDATB- β -CD was placed into a quartz crucible in the PVD chamber that was then

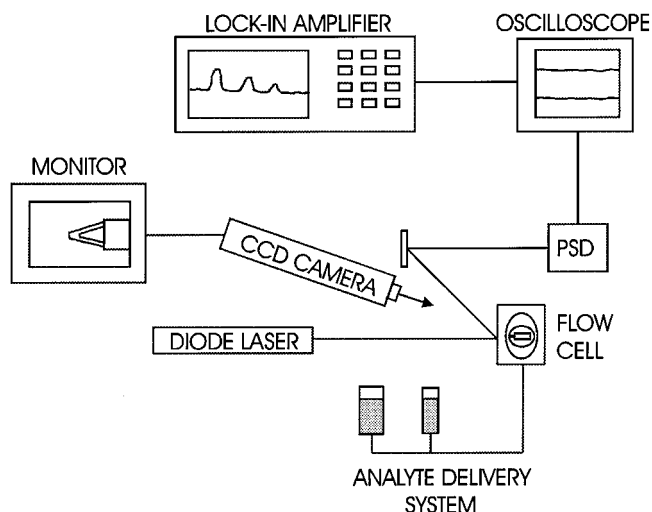


Figure 3. Schematic representation of the instrumentation used for cantilever measurements. A position-sensitive detector (PSD) was used to monitor deflections of laser beam reflected from MC surface. The MC-containing flow cell was composed of Teflon and had a fixed volume of $\sim 100\text{ }\mu\text{L}$. The analyte delivery system consisted of two syringes connected in series using 2-way valves.

electrically heated in a vacuum, causing the cyclodextrin to evaporate onto the MC surface. The thickness of the resulting film was measured using a conventional quartz crystal microbalance (Maxtek, model TM-100R, Santa Fe Springs, CA). Vapor-deposited films with QCM-based thicknesses of ~ 18 and 50 nm were used. With both types of chemically modified cantilevers, the cantilever was allowed to equilibrate in the background solution until a stable baseline was achieved before any measurements were attempted.

The deflection of the MC was measured using an optical beam-bending technique (Figure 3). In this technique, deflection of the cantilever is measured by reflecting a 5 mW diode laser (Coherent Laser Corp., Auburn, CA) operating at 632 nm off of the tip of the MC and onto a position sensitive detector (built in house).¹⁹ The output of the detector was recorded and stored using a SRS 850 DSP lock-in amplifier as a digital recorder (Stanford Research Systems, Sunnyvale, CA). The conversion factor for converting output voltage to MC deflection was determined by displacing the detector using a micrometer and measuring the resulting change in output voltage. The output signal was fed through a TDS 220 digital oscilloscope (Tektronix, Beaverton, OR) to facilitate optical alignment. The MC flow cell was imaged using a Wattec CCD camera for alignment of the laser beam on the cantilever tip (Edmund Industrial Optics, Barrington, NJ). The readout accuracy of our system was $\sim 0.25\text{ nm}$, and the noise associated with the measurement under flow was $< 10\text{ nm}$ in most experiments. The MC was mounted in a $100\text{-}\mu\text{L}$ Teflon flow cell and exposed to various solutions at a flow rate of 0.85 mL/min. The analytes were delivered to the cell via a 10-mL syringe connected to a 2-way valve. This valve was placed in series with a second 2-way valve connected to a 50-mL syringe that was used to flow background solution into the cell. The analytes were diluted in the syringe using the flowing background solution that was a 0.025 M phosphate buffer at pH 7 to ensure the analyte solution was at thermal equilibrium with the background solution. Mea-

surement of pH was performed using an Orion SA 520 pH meter (Thermo Orion, Beverly, MA).

Film and MC surface characterization was performed using both spectroscopic and surface imaging techniques. Spectroscopic information was obtained using C^{13} nuclear magnetic resonance spectroscopy (NMR), Fourier Transform infrared spectroscopy (FT-IR), and X-ray photoelectron spectroscopy (XPS). Surface images were obtained using atomic force microscopy (AFM). The NMR experiments were performed using a Varian Mercury 300 MHz NMR spectrometer (Varian Inc., Palo Alto, CA); the FT-IR experiments, using a Bio-Rad FTS-60A infrared spectrometer (Bio-Rad, Hercules, CA); the AFM images were obtained using the tapping mode of a Digital Instruments Multimode AFM (Digital Instruments, Santa Barbara, CA); and the XPS spectra were obtained using a Perkin-Elmer PHI 5000 series ESCA (Perkin-Elmer, Wellesley, MA).

The metals used in the coating process of the cantilevers were purchased from Alfa Aesar (Ward Hill, MA) or the Kurt J. Lesker Company (Livermore, CA) at a purity of 99.9%. The analytes and buffer components used were obtained from Sigma (St. Louis, MO) or Aldrich (Milwaukee, WI) and were used as received. All acids and bases used were obtained from Fisher Scientific (Pittsburgh, PA). Ultrapure water was obtained by using a Barnstead E-Pure water filtration system (Barnstead, Dubuque, IA). The HM- β -CD was synthesized using the method of Stoddart et al.,²⁵ and the HDATB- β -CD was synthesized using the method of Takeo et al.²⁶ All buffer solutions consisted of monobasic and dibasic sodium phosphate dissolved in ultrapure water. The ratio of the two components was fixed to yield a buffer at pH 7. All analyte solutions were prepared in this buffer solution that is also called the background solution.

RESULTS AND DISCUSSION

Surface Modification and Characterization. We have applied chemical coatings to different MC surfaces in an attempt to study the effect of morphology on sensor response. Nanostructuring the cantilever surface creates three important results: a larger surface area compared to a MC with the same geometric area, spatially confined spaces, and stabilization of thicker films applied to its surface. In some cases, the nanostructuring itself has led to slight changes in selectivity for gas-phase measurements based upon the size of the features and the analyte.²³ To study these effects for liquid-phase measurements, we have exposed these various MCs to aqueous solutions of a set of analytes previously observed to reversibly interact with β -CD cavitands. We have chosen to use cyclodextrin macrocycle sugar cavitands as chemical coatings because of their established molecular recognition capabilities. Solutes interact with CDs on the basis of size, geometry, and physiochemical properties of both the solute and CD.²⁷ These unique interactions have resulted in high levels of selectivity in chemical separations.^{28–31} However, in chemical

sensor work in which the CD is covalently bound or deposited on a surface as a disordered film, the molecular recognition properties of the CD may be altered. We have used a thiolated cyclodextrin (HM- β -CD) and one that was thermally evaporated in a vacuum (HDATB- β -CD) as our chemical coatings. To our knowledge, this is the first use of a thermally evaporated cyclodextrin film as a chemical sensor coating.

Although direct spectroscopic investigations of the HM- β -CD-gold MC surface were not performed, prior reports of thiolated-CD binding to gold^{32,33} and certain experiments we performed indicate that a substantial chemically attached layer of HM- β -CD was formed on the gold surface following treatment with pure solutions of the thiolated CD. Previously performed XPS measurements confirm the presence of sulfur on the surface after treatment with HM- β -CD. In addition, the contact angle for water on these surfaces was substantially altered. When the responses of an untreated and a HM- β -CD treated MC to the certain analytes were compared, the response of the former (sorption onto the active gold surface) was irreversible, whereas the response of the HM- β -CD-treated cantilever was reversible. The response of the MC to pH was also measured before and after treatment with HM- β -CD. Upon treatment of the MC with HM- β -CD, there was a considerable decrease in response to pH, again indicating that the surface was modified with a chemical layer.

As a result of the fact that HDATB- β -CD was thermally evaporated onto the cantilever surface, it was important to determine if the compound decomposed during the evaporation process. Both C^{13} NMR and FT-IR spectroscopy were used to characterize the compound before and after vapor deposition. For the reference comparison, a solution of HDATB- β -CD was prepared in bulk, and the C^{13} NMR spectrum was obtained. A small droplet of this solution was placed onto a gold-coated microscope slide and allowed to dry. The surface was measured using FT-IR. Subsequently, thin films were vacuum-vapor-deposited onto a gold-coated microscope slide and measured as above. A C^{13} NMR spectrum was obtained by dissolving the vapor-deposited film from the surface and measuring the resulting solution. The NMR experiments showed that within experimental error, the film was the same before and after the vapor deposition process. The C^{13} peaks in the spectra (before; after) for the most prominent bonds were as follows: C=O (170.5, 169.2; 170.8, 169.5), C-1 (96.5; 96.5), C-4 (75.0; 75.2), C-2,3,5 (71.6, 71.2, 71.0; 71.8, 71.5, 71.2), C-6 (61.8; 61.8), $(CH_3)_3C$ (25.9; 25.8), $COCH_3$ (20.9, 20.7; 20.9, 20.8), and $(CH_3)_2Si$ (-4.9, -5.2; -5.0, -5.3). There were very small shifts in peak positions due to instrumental variations. However, it should be noted that some of the relative intensities of the peaks did change. This may be due to the loss of an impurity during the vaporization process. Figure 4 shows that the FT-IR spectra for physical (a) and vacuum vapor deposition (b) are nearly identical. The lack of bands in the region 1700–1500 cm^{-1} for the vapor-deposited sample is probably due to a loss of a nonvolatile contaminant present in the bulk material. These bands in the 1700–1500 cm^{-1} region are relatively weak and do not correspond well with any known bonds in the CD compound. The reaction scheme to produce the HDATB- β -CD

(25) Rojas, M. T.; Koniger, R.; Stoddart, J. F.; Kaifer, A. E. *J. Am. Chem. Soc.* **1995**, *117*, 336.

(26) Takeo, K.; Mitoh, H.; Uemura, K. *Carbohydr. Res.* **1989**, *187*, 203–221.

(27) Fox, S. B.; Culha, M.; Sepaniak, M. J. *J. Liq. Chromatogr. Relat. Technol.* **2001**, *24*, 1209–1228.

(28) Copper, C. L.; Davis, J. B.; Cole, R. O.; Sepaniak, M. J. *Electrophoresis* **1994**, *15*, 785.

(29) Copper, C. L.; Davis, J. B.; Sepaniak, M. J. *Chirality* **1995**, *7*, 401.

(30) Lelièvre, F.; Gareil, P.; Jardy, A. *Anal. Chem.* **1997**, *69*, 385–392.

(31) Culha, M.; Fox, S.; Sepaniak, M. J. *Anal. Chem.* **2000**, *72*, 88–95.

(32) Weisser, M.; Nelles, G.; Wenz, G.; Mittler-Neher, S. *Sens. Actuators B* **1997**, *38–39*, 58–67.

(33) Lee, J.-Y.; Park, S.-M. *J. Phys. Chem. B* **1998**, *102*, 9940–9945.

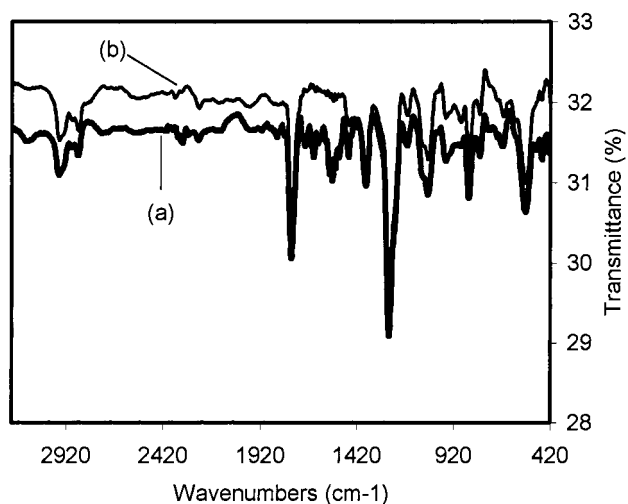


Figure 4. IR spectra of HDATB- β -CD before (a) and after (b) vapor deposition onto a gold-coated surface.

involves several steps and chromatographic isolation of the desired product, but clearly not in the highest purity.²⁵ It should be noted that CDs similarly functionalized at the C2, C3, and C6 hydroxyl positions have been used as stationary phases in gas chromatography at temperatures ranging up to 200 °C.^{34,35}

Both AFM and XPS were used to study the thin film coated MCs. Figure 5 shows the AFM images (left) and XPS spectra (right) for three of the surfaces studied. The AFM images ($1 \times 1 \mu\text{m}$) were obtained from an actual cantilever surface and show a colloidal type surface for the uncoated nanostructured surface as well as for the surface coated with the 18-nm film of HDATB- β -CD. The root-mean-square (rms) roughness of the bare nanostructured surface in Figure 5 (top) is ~ 30 nm. There is an apparent reduction in particle size upon addition of the thin (18 nm) film (rms roughness, 20 nm). This may be due to a filling in of the crevices between colloidal particles of gold or the buildup of small CD aggregates on top of colloidal particles. In either case, it is likely there are areas where there is bare metal or a very thin (<5 nm) film on the surface. The thicker (50 nm) film (rms roughness, 18 nm) shows an increase both in the size of the features and in the continuity of the features, presumably due to a complete but not smooth coverage of the nanostructured surface. Further evidence of this can be seen in the XPS spectra of the surfaces. The XPS spectrum of the bare nanostructured surface was obtained from a gold-coated microscope slide and shows both gold and silver peaks as a result of the presence of these metals in the coating. There is also a small amount of carbon and oxygen present due to adsorbed hydrocarbons. Upon addition of the 18-nm CD film, the gold and silver peaks are greatly diminished, whereas the carbon and oxygen peaks show a considerable increase. There is also the presence of silicon on the surface because of the silicon in the CD. Small peaks due to gold present in the spectrum of the 18-nm-coated surface indicates that there is not a complete coverage of the metallic layer by the thin film. In comparison, the metal peaks are essentially absent in the

spectrum of the nanostructured surface coated with the 50-nm film, indicating that the underlying metallic layer is more completely covered.

Control Experiments. Control experiments were performed in order to verify that the observed responses were principally due to the analyte binding with the chemically modified side of the MCs. For our purposes, tensile and compressive responses will be defined as bending away from and bending toward the silicon nitride side of the MC, respectively. Responses to each analyte were obtained for both smooth and nanostructured cantilevers that were not chemically modified with cyclodextrins. Upon exposure to each analyte at the highest concentrations used in our studies, the uncoated MCs exhibited a compressive response of no more than 50 nm for the dihydroxynaphthalene (DHN) series and 20 nm for the other analytes. These responses were in the same deflection direction as for chemically modified MCs but were far smaller in magnitude (see below). The observed blank responses were the greatest for the nanostructured surface, with the responses for the smooth surface being barely detectable. In some cases, the small blank responses were not reversible.

The pH responses of nonchemically modified cantilevers were also investigated. For a smooth gold surface, tensile responses were observed for pH values <7 and compressive responses for pH values >7 . The average value of cantilever deflection was ~ 90 nm/pH unit at pH 7, which corresponds well with previous work done by Thundat and co-workers.³ When making these same measurements with a nanostructured surface, the results were quite different. Compressive responses were observed for pH values <7 and tensile responses for pH values >7 . The average value of cantilever deflection for this system was ~ 500 nm/pH unit at pH 7. It is logical to surmise that increases in pH response with nanostructuring are related to increases in surface area, although the response characteristics, including the change in deflection direction, may also reflect a different chemical nature of the nanostructured surface that results from the dealloying procedure. Differences in response for smooth versus nanostructured MCs indicate the importance of analyte interactions with the active side but do not preclude the possibility of some interaction with the silicon nitride side. An ability to overwhelm interactions with the nontreated side of the MCs with very large stresses on the nanostructured side is another advantage of our approach.

Finally, control experiments were performed to gauge the effect of solute-induced changes in refractive index (RI) on the responses of our system. In this work, the incident and reflected laser beams traverse RI barriers at angles near normal; therefore, refraction effects are small. In addition, it should be realized that reflection at the MC in our optical arrangement does not occur on the receptor or nanostructured side. As a result of reflectance from the base of our MC chips, we observed a small (30–40 nm) compressive deflection when going from pure water to our 25 mM buffer and essentially no detectable deflection when the buffer was then made to contain the highest 2,3-DHN concentration employed. Deflection measurements reported herein were performed with the plane of the incident and reflected beam in the same plane as Δz . With our apparatus, the post that holds the MC can be rotated 180° to reverse the direction of cantilever deflection without changing any possible RI effect. Using the

(34) Bicchi, C.; Cravotto, G.; D'Amato, A.; Rubiolo, P.; Galli, A.; Galli, M. *J. Microcolumn Sep.* **1999**, *11*, 487–500.

(35) Beck, T.; Liepe, J.-M.; Nandzik, J.; Rohn, S.; Mosandl, A. *J. High Resolut. Chromatogr.* **2000**, *23*, 569–575.

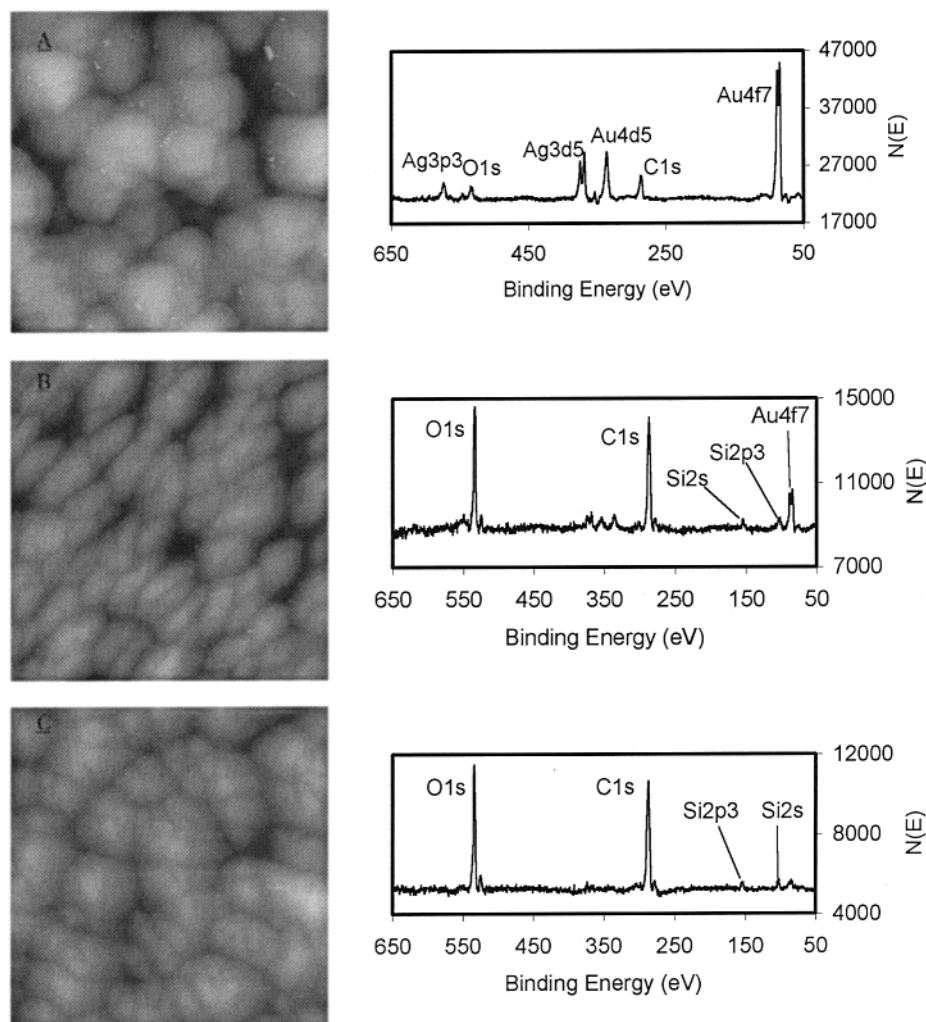


Figure 5. Atomic force microscopy images (left column) and X-ray photoelectron spectra (right column) of a nanostructured surface (top), a nanostructured surface coated with 18 nm of HDATB- β -CD (middle), and a nanostructured surface coated with 50 nm of HDATB- β -CD (bottom). The AFM images are based on a $1 \times 1 \mu\text{m}$ scan. The maximum height (seen as white) for each image is 300 nm.

nanostructured MC with an 18-nm film of HDATB- β -CD (see below), the response to the highest concentration of 2,3-DHN was found to maintain the same magnitude of signal (within 10%) but change direction when the 180° rotation was performed. It is clear that the signals reported in this work involve negligible contributions due to RI effects, even at the highest analyte concentrations. In fact, a unique optical configuration is possible with our system. The cantilever can be rotated to a 90° configuration that places deflections of the cantilever in a vertical plane (see Figure 6a) and RI effects in the horizontal plane (see Figure 6b) at the PSD. Since the vertical and horizontal outputs of the PSD are separately available for processing, the two effects (true signal and RI artifacts) can be distinguished.

Deflection Measurements. Different types of films and film thicknesses were used on both smooth and nanostructured MCs to study their influence on MC response. When comparing a smooth to a nanostructured MC surface, an increase in the available binding sites in rough proportion to the increase in surface area is expected. In addition to an increase in the total energy of binding due to more binding events, the strong short-range intermolecular forces occurring for receptors and analytes located in narrow crevices^{20–22} on the structure may yield a more

efficient conversion of the energy of binding into cantilever bending. This unique feature allows for enhancements in bending greater than the increase in surface area. In prior gas-phase work, it was determined that a 50-nm-thick dealloyed surface has roughly a 17-fold greater surface area than a smooth gold surface, but exhibited enhancements in response in some cases that were ~ 100 -fold.²³ An objective of the work reported herein was to determine if liquid-phase systems, in which the organic receptor phase is highly solvated, yield similar enhancements in chemi-mechanical response due to nanostructuring.

Self-assembled monolayers of HM- β -CD were formed on both smooth and nanostructured MCs. Cantilever deflections were measured on both MC systems for the set of analytes. Figure 7 shows the response of the two different surfaces to 2,3-DHN. The compressive response of the nanostructured MC is ~ 4.5 times larger than that of the smooth one for a 10-fold less concentrated solution. This general trend (larger response on a nanostructured surface) is true of all of the analytes we studied. In addition, the molecular recognition properties of the CD can be seen. The larger molecules (DHNs) exhibit larger responses and lower limits of detection (LODs) than the other molecules studied, for which the LOD is determined to be a signal-to-noise ratio of 3 for

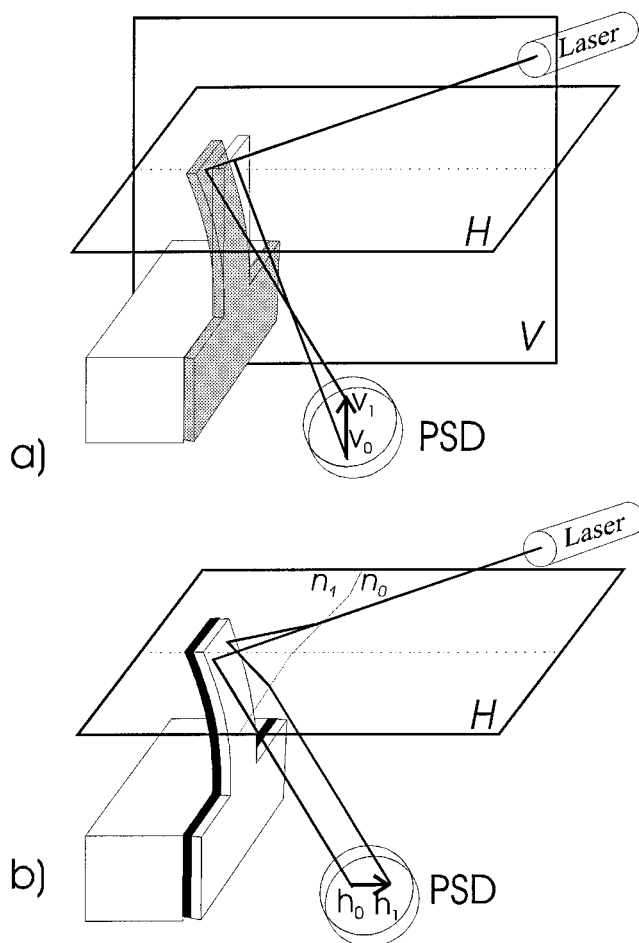


Figure 6. Depiction of 90° optical arrangement that places MC bending deflections and refractive index deflections in orthogonal planes at the position sensitive detector (PSD).

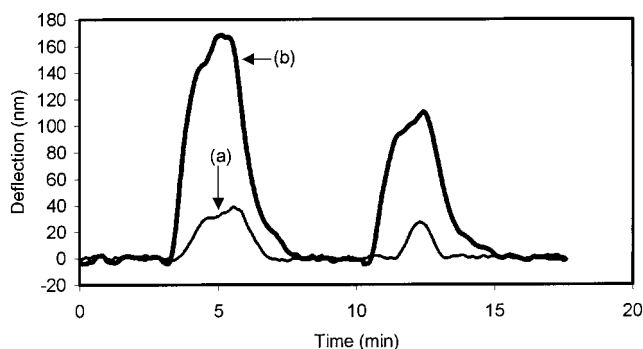


Figure 7. Response to 2,3-DHN of a HM- β -CD-treated smooth (a) and nanostructured (b) MC. The responses shown are for 1000 and 500 ppm (a) and 100 and 50 ppm (b) analyte concentration in a 0.025 M, pH 7 phosphate buffer. The calculated LODs were 290 and 4.80 ppm for the smooth and nanostructured MCs, respectively.

MC bending (see Table 1). This may be explained by higher binding constants for the larger two-fused-ring DHN molecules relative to the other single-ring analytes. The two-fused-ring systems exhibit a better “snug” fit into the cavity of β -CD; evidence of this can be found in our prior work involving cyclodextrins as running buffer additives in capillary electrophoresis and in molecular modeling studies.^{27,29,31} However, since measurements are based on stress changes, response differences between these classes of analytes may be related to differences in intermolecular

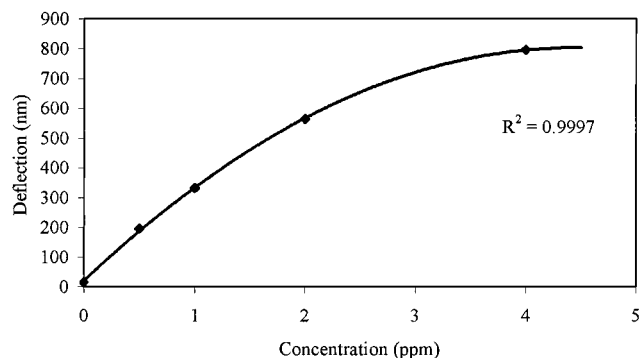


Figure 8. Concentration-based deflection of a nanostructured MC modified with a 50-nm film of HDATB- β -CD exposed to 1,7-dihydroxynaphthalene.

forces that are not directly related to binding constants. For example, one can envision interactions between the aromatic groups of opposing DHNs bridging across deep crevices that contribute to the stresses observed in these studies. The LODs for all of the analytes range from 242 to 1.50×10^3 ppm and from 4.80 to 144 ppm on the smooth and nanostructured surfaces, respectively. The average improvements in LOD upon nanostructuring for the DHNs and other compounds were 40 and 13, respectively, demonstrating that substantial enhancements in performance can be realized for liquid-phase measurements.

The concept of analyte-induced modulation of the surface free energy of SAM functionalized MC surfaces, as a means to stress and bend the surfaces, is rendered fuzzy with nanostructuring and may be best described by theories describing stresses in colloidal systems.²⁰ In the case of thin films on those structures, the mechanism of stress is completely different. Analyte-induced swelling of the film leads to bending by a mechanism more akin to that observed in bimetallic devices with the two metals exhibiting different coefficients of thermal expansion.²⁰ However, thin organic films applied to smooth MC surfaces that swell with analyte absorption may “slip” or move along the surface to minimize stress. This reduces the response of the cantilever. There may also be reduced adhesion when applying films to a smooth surface. When applying films to a nanostructured surface, the phase is effectively anchored, and the amount of slippage should be reduced. We have used films of thermally evaporated HDATB- β -CD that allow for facile adjustment of film thickness, even on diminutive MCs. When 18-nm-thick HDATB- β -CD films were applied to both smooth and nanostructured MCs, the observed LODs for all of the analytes were substantially lower for the nanostructured MC (see Table 1). The average improvements in LODs were 25 and 9 for the DHNs and other compounds, respectively. This suggests that by using the nanostructured surface, the stress generated by film swelling was more effectively translated into MC bending.

It is interesting to note that the overall performance of the nanostructured SAM MC is better than the nanostructured 18 nm film MC. These systems differ in the disposition of CD on the surface, the actual type of CD, and the mechanism of analyte-induced bending. These factors make it difficult to compare selectivity patterns achieved on these cantilevers. However, it is important to note the achieved increase in sensitivity in going from a smooth surface to a nanostructured surface. It was decided to

Table 1. Observed Limits of Detection^a for the Analytes Measured on the Various Surfaces

compd	SAM		17-nm		50 nm, nanostructured
	smooth	nanostructured	smooth	nanostructured	
2,3-DHN	288	4.80	31.3	0.988	0.0248
1,7-DHN	242	8.50	22.4	4.45	0.0383
2,7-DHN	250	7.50	39.5	1.02	0.0387
tolazoline	300	17.0	214	13.1	4.87
ephedrine	326	31.3	93.8	15.7	14.4
benzoic acid	1.50×10^3	144	250	42.1	18.3

^a LODs were calculated using a signal-to-noise ratio of 3. A typical value of the noise was 7 nm. All values listed in the table are given in terms of parts per million (ppm).

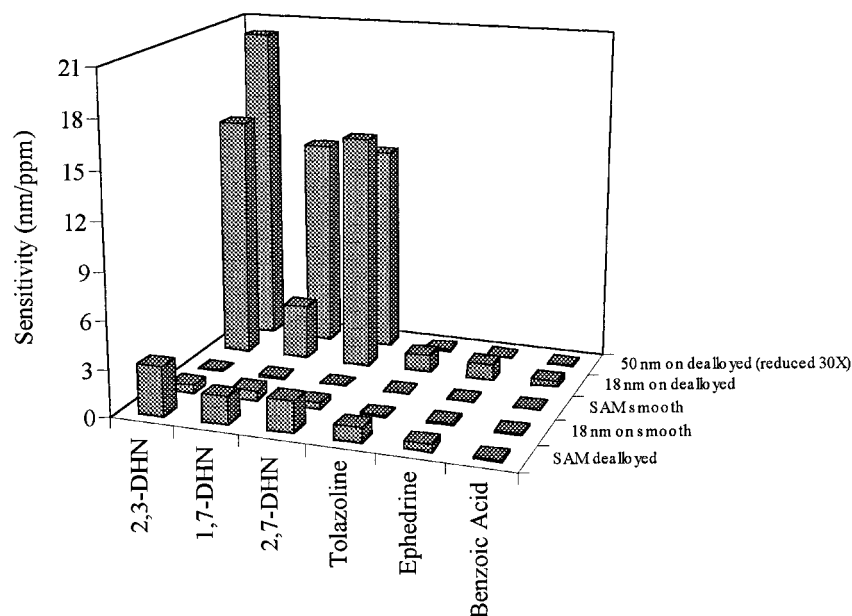


Figure 9. Comparison of the observed sensitivities for each analyte on the various surfaces studied. The values for the 50-nm-thick film of HDATB- β -CD have been reduced by a factor of 30 for the nanostructured surface.

investigate two film thickness regimes, substantially less than and greater than the rms roughness of the bare nanostructured surface. The fact that these produce different surfaces was demonstrated in conjunction with Figure 5. We surmise that swelling of the thin (probably discontinuous) 18-nm film within the nanostructured surface may have a large out-of-plane (of the MC) component that is not effectively translated into in-plane stress. For this reason, thicker (continuous) films should be, and generally are, used.^{5,12,36}

In a previous work, we created relatively thick (50–500 nm) coatings of GC phases on smooth MC surfaces using a spin-coating technique.¹⁰ The largest responses to gas-phase analytes were obtained with the thinnest (50 nm) films. The loss in response with greater film thickness may have been due to stress-induced slippage. However, since the measurements were not performed under true equilibrium conditions, it also could have been due to slow kinetics. Although it is true that the mass loading of analyte increases with film thickness, bending due to increased mass is generally much smaller than that due to in-plane stress. It is for this reason that we have chosen to use a very well

controlled vacuum vapor deposition approach to deposit very thin to moderately thick layers of receptor phases on MC surfaces. Despite having only limited quantities of HDATB- β -CD, we were able to compare films with a thickness of 18 and 50 nm. As can be seen in Table 1, the 50-nm film performed much better (an average factor of 60 better than the 18-nm film for the DHNs). This film appears to be more continuous than the 18-nm film, as seen in Figure 5 (bottom), leading to efficient conversion of swelling to in-plane stress. With our flow system, the response kinetics for the 50-nm film MC was essentially the same as seen in Figure 7 for the SAM MC.

Figure 8 shows a calibration plot of the 50-nm-thick HDATB- β -CD film exposed to 1,7-DHN. The system exhibits the response typical of a Langmuir type film, with the onset of saturation between 2 and 4 ppm. However, even at low concentrations, the response is relatively large, with a very high sensitivity. The sensitivity to each analyte as a function of film type and cantilever morphology can be seen in Figure 9. The highest sensitivity is achieved on the nanostructured cantilever modified with the 50-nm film of HDATB- β -CD. This indicates that using a nanostructured surface with a thicker chemical coating can greatly enhance sensor performance. It is also evident that all of the films on the nanostructured cantilevers performed better than any of the films

(36) Battiston, F. M.; Ramseyer, J.-P.; Lang, H. P.; Baller, M. K.; Gerber, C.; Gimzewski, J. K.; Meyer, E.; Güntherodt, H.-J. *Sens. Actuators B* **2001**, 77, 122–131.

on a smooth cantilever. Given the wide range of polymeric and other films that are widely used and characterized, this appears to be a significant finding. The films on smooth cantilevers were marked by very low sensitivities and relatively higher LODs. The LODs obtained on the 50-nm film on a nanostructured MC were in the parts-per-billion range for the DHNs. The relative standard deviation tested via replicate ($n = 8$) consecutive measurements of a solution of 100 ppm DHN was 11% on day 1 and 9% on day 2. The average value in deflection from day 1 was $\sim 76\%$ of the average value from day 2. Thus, reasonable reproducibility is possible with this nondifferential system, but calibration should be performed on at least a daily basis.

It can be envisioned that MC arrays can be made in this same general manner. Using vapor deposition and suitable masks, it should be possible to individually coat MCs in an array. Increasing film thickness may prove to enhance sensor performance even

further than what we have demonstrated in this work. In addition, the larger responses achieved using nanostructured cantilevers with thick films may prove advantageous in the development of chemi-mechanical MC actuators.

ACKNOWLEDGMENT

We thank Dr. Tom Green for synthesizing the HM- β -CD used in these studies and James Corbeil for his help in obtaining the AFM images. This research was supported by the U.S. Department of Energy, Environmental Management Program under Grant DOE DE-FG07-98ER62718 and by the DOE Basic Energy Sciences under Grant DE-FG02-96ER14609.

Received for review February 4, 2002. Accepted April 8, 2002.

AC020074O